1995

Diagnostics of CdTe Electrodeposition by Rest Potential Voltammetry

Brandon Kemp
Arkansas State University

Robert Engelken
Arkansas State University

Arif Raza
Arkansas State University

Arees Siddiqui
Arkansas State University

Omer Mustafa
Arkansas State University

Recommended Citation

Kemp, Brandon; Engelken, Robert; Raza, Arif; Siddiqui, Arees; and Mustafa, Omer (1995) "Diagnostics of CdTe Electrodeposition by Rest Potential Voltammetry," *Journal of the Arkansas Academy of Science*: Vol. 49 , Article 21.
Available at: http://scholarworks.uark.edu/jaas/vol49/iss1/21

Diagnostics of CdTe Electrodeposition
by Rest Potential Voltammetry

Brandon Kemp, Robert Engelken, Arif Raza, Arees Siddiqui and Omer Mustafa
Optoelectronic Materials Research Laboratory
Department of Engineering
Arkansas State University
P.O. Box 1740
State University, AR 72467

Abstract

Due to the extreme sensitivity of the partial elemental currents (i.e., i_{Cd}, i_{Te}) and, hence, stoichiometry to deposition voltage, temperature, mass transport, and ambient light intensity during electrodeposition of semiconductor films, it is important to implement *in-situ* methods for monitoring the stoichiometry and related semiconductor efficacy of the growing film. We report investigation of open circuit rest potential (E_{oc}) voltammetry as one such method during electrodeposition of CdTe from aprotic electrolytes such as ethylene glycol. Plots of transient open circuit potential versus sweep voltage exhibit distinct transition and plateau structures corresponding to Te, CdTe, and Cd phases and correlating with the appearance/disappearance of photocurrent, x-ray diffraction evidence of the three phases, and optical obsorption spectroscopy. In particular, the E_{oc} plateau corresponding to deposition of near-stoichiometric CdTe can be used to monitor and control the deposition process.

Introduction

Cadmium telluride (and sister compounds $Hg_{1-x}Cd_xTe$, $Cd_{1-x}Zn_xTe$, and $Cd_{1-x}Mn_xTe$) has become one of the most valuable and most investigated semiconductor compounds because of its potential application in a variety of systems and devices, for example, photovoltaic energy conversion and light detection. Electrodeposition has emerged as one of the more interesting methods for depositing compound semiconductor thin films because of obvious advantages, including low chemical and equipment costs, low temperature and atmosphere pressure operation, potential to be scaled up to large areas, and convenient monitoring and control through its electrical nature. However, a better understanding of the chemistry/electrochemistry is needed for more precise control of this process.

Experimental results have been reported describing the electrochemical deposition and subsequent material characteristics of CdTe (Sella et al., 1986), (Verbrugge and Tobias, 1987), (Von Windheim and Cocivera, 1991) and its sister compounds such as $Hg_{1-x}Cd_xTe$ (Mori et al., 1990) and CdSe (Ham et al., 1991). Photovoltaic properties of CdTe-based devices also continue to be investigated (Kim et al., 1994). Still, theoretical models (Engelken and Van Doren, 1985), (Engelken, 1987), (Engelken, 1988) describing solution electrochemistry provide an understanding of the CdTe codeposition process.

The quasi-rest potential (QRP) has been defined as the open circuit potential established immediately after current interruption and before there has been any relaxation of nonequilibrium ion concentrations at the cathode surface due to diffusion effects (Engelken, 1987). E_{oc} is heavily dependent upon ion concentrations, cathode surface stoichiometry, and temperature, as governed by the mixed reversible potential dictated by zero total current. It is determined, ideally in the absence of other interfering species such as H^+, by the voltages which makes the partial tellurium and cadmium currents negatives of each other in the Butler-Volmer/Tafel current-potential characteristics for each ion. Eventually, ion relaxation and changes in the CdTe surface to Te-richness due to exchange of Te(IV) for Cd(II) will transform the QRP to the equilibrium rest potential described by equating the Nernst Potentials for both Te and Cd:

$$E_{oc} = E^o - (RT/nF) \ln [a_M/a_M(+n)] \quad (1)$$

where E^o is the standard reduction potential, R the universal gas constant, n the ionic charge, F Faraday's constant, T the Kelvin temperature, a_M the elemental activity, and $a_M(+n)$ the activity of the ions in solution for a pure elemental electrode in a solution of its positive-valent ions. In an intermetallic compound, such as CdTe, modeled by

$$Cd_{(s)} + Te_{(s)} = CdTe_{(s)} \quad (2)$$
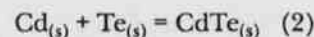
the activities of the constituent elements are reduced to the bonding between the atoms according to the equilibrium constant expression

$$a_{CdTe}/(a_{Cd}a_{Te}) = exp[-\Delta G^o/(RT)] \quad (3)$$

where ΔG^o is the Gibb's free energy for CdTe formation (Engelken, 1988).

The described work focused on characterization of organic solutions used for CdTe electrodeposition in search of convenient and low cost monitoring of thin film stoichiometry. It is hoped that measurements of open circuit potential (E_{oc}) will provide information on the electrochemical nature of the solution as well as composition of growing films. This paper will present data relating the open circuit potential of electrodeposited CdTe thin films to some of the controlling variables such as Te(IV) concentration, deposition voltage, and illumination.

Materials and Methods

The equipment used in film deposition and to measure E_{oc} included 1 cm^2 indium-tin oxide (ITO) coated glass cathodes (Balzers and Donnelly) held by a Poco graphite cathode clamp utilizing Teflon bolts and nuts. A Fisher Ag/AgCl reference electrode was utilized. A Poco graphite anode was used with 3 cm^2 submerged. The E_{oc} versus E_{sweep} plots were obtained using an EG&G Princeton Applied Research Model 362 scanning potentiostat and a Hewlett Packard 7046-B x-y recorder. Other items in solution were a Teflon covered stirring bar and a Fisher Hg-filled thermometer.

The Alfa/Johnson Matthey ethylene glycol (99$^+$%) solutions contained 0.05 M Aldrich reagent grade CdCl$_2$ and 10^{-4} to 10^{-3} M Alfa/Johnson Matthey 99.9% TeCl$_4$. The solvents were quickly dissolved by heating the solution to 40°C.

A Rigaku D-MAX x-ray diffractometer (XRD) and a Perkin-Elmer Lambda 19 UV/VIS/NIR optical spectrophotometer were used in film characterization.

The ITO glass substrates were cleaned using Comet cleanser and tap water. This was followed by distilled water rinsing and drying under an air stream.

The solution was heated to 100°C. The E_{oc} versus E_{sweep} plots were then obtained at a sweep rate of 1 mv/s or 2 mv/s for sweeps accompanied by pulsed illumination. The on/off current times were controlled at 3-4 s by an in-house built pulser circuit. Current (I) versus E_{sweep} plots were obtained at a sweep rate of 5 mv/s. Pulsed illumination accompanied I versus E_{sweep} plots with equal on/off times of about 2.5 s. Longer on/off times (i.e. about 15 s each) were used for illuminated potential sweeps to compensate for the slower sweep rate. Film depositions were then performed using fresh ITO glass substrates. The films were rinsed in hot ethylene glycol followed by hot distilled water. The films were then placed in an air stream to dry, prior to XRD and spec-trophotometer characterization.

Results and Discussion

As predicted, a direct correlation between E_{oc} and deposition voltage was observed in the potential plots. Three distinct plateau structures were seen in E_{oc} versus E_{sweep} plots indicating different E_{oc} values corresponding to Te, CdTe, and Cd.

Figure 1 exhibits the E_{oc} versus E_{sweep} plot for a solution containing $3 \cdot 10^{-4}$ M TeCl$_4$. Notice the transition from the first structure (A) corresponding to deposition of elemental tellurium to the middle plateau region at a sweep potential of about -0.20 V. This level plateau (B) corresponds to the regions in which CdTe is plated and in which photocurrents were observed on the corresponding photovoltammogram (Fig. 2). Another transition region (C), observed at about -0.70 V, corresponds to Cd plating on the I versus E_{sweep} plot. Figure 3 shows XRD data for a film deposited at -0.60 V from this solution. Strong diffraction peaks match the vertical CdTe powder diffraction file lines. Figure 4 is a plot of optical absorbance versus wavelength for the same film. Notice the deflection (absorption edge) near 800 nm. This is consistent with the 1.45 eV direct bandgap of CdTe. The "hump" centered near 1300 nm is an interference ripple caused by interference in the film as wavelength is varied.

The next data set reveals results of pulsed illumination on an E_{oc} versus E_{sweep} plot (Fig. 5) for a similar solution containing $4 \cdot 10^{-4}$ M TeCl$_4$. The photovoltages occur in the same sweep voltage range (i.e. from -0.30 V to -0.70 V) as the photocurrents on the forward sweep of the corresponding cyclic voltammogram (Fig. 6). Figure 7 presents XRD data for a film deposited at -0.65 V from this solution. Strong diffraction peaks match CdTe file peak locations, an indication of polycrystalline CdTe deposition Figure 8 shows spectrophotometer data for the same film. Again, a deflection of the curve occurs as a wavelength near 800 nm. However, a narrow tail preceding this deflection could indicate slight Cd - richness in film composition. This is consistent with the open circuit curve which shows a region of transition to the E_{oc} of metallic Cd just negative of the "knee" at the -0.65 V deposition voltage.

Figure 9 is an E_{oc} versus E_{sweep} plot for a solution with a TeCl$_4$ concentration of $7 \cdot 10^{-4}$ M. The plateau structures persist for this high [Te(IV)] solution, but are shifted negative with respect to similar structures for lower [Te(IV)] solutions. The I versus E_{sweep} voltametric structures, plotted in Fig. 10, are also shifted negative. A film, deposited at a more negative voltage than those previously discussed (i.e. at -0.85 V), produced XRD and spectrophotometer data exhibited in Fig. 11 and Fig. 12,
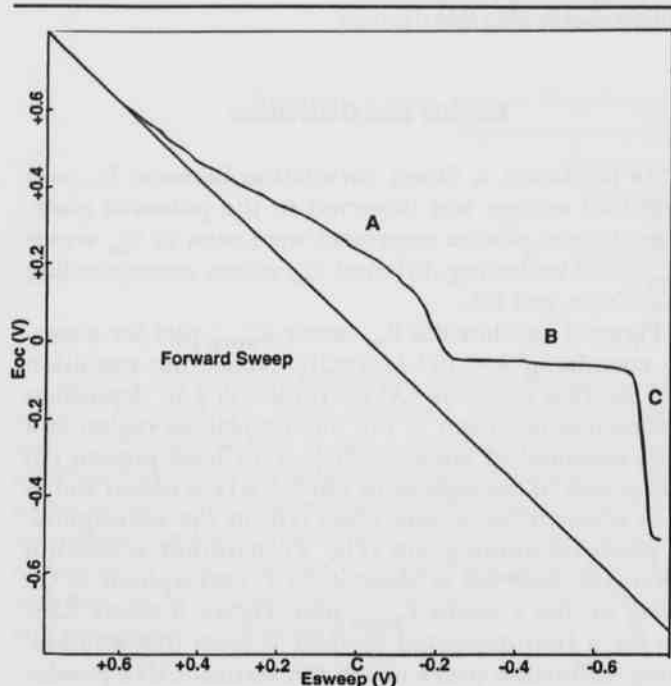
Brandon Kemp, Robert Engelken, Arif Raza, Arees Siddiqui and Omer Mustafa

Fig. 1. E_{oc} vs. E_{sweep} curve for a solution containing $3 \cdot 10^{-4}$ M $TeCl_4$ and 0.05 M $CdCl_2$ in ethylene glycol at 100°C. Note the three structures, A, B, and C, corresponding to elemental Te, CdTe, and Cd metal, respectively.
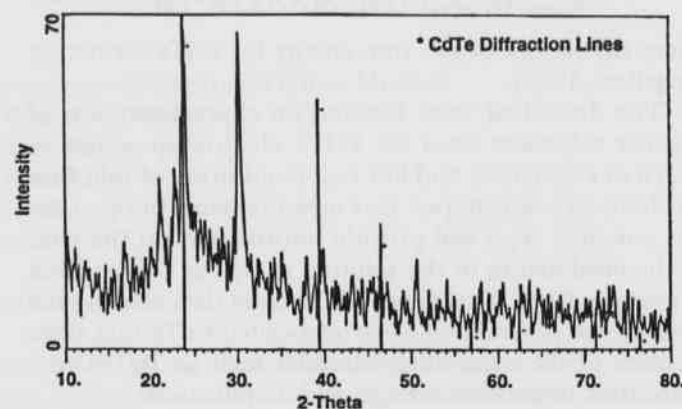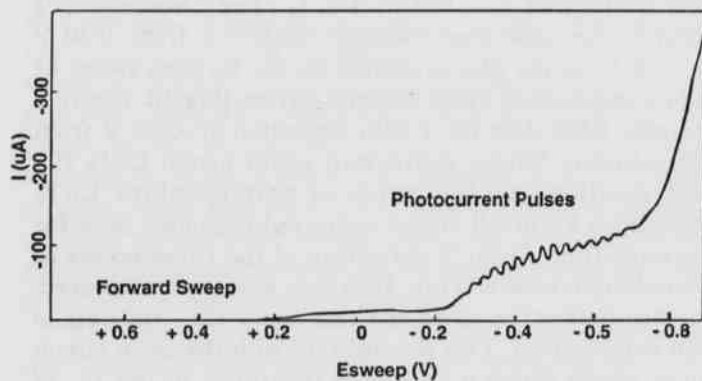

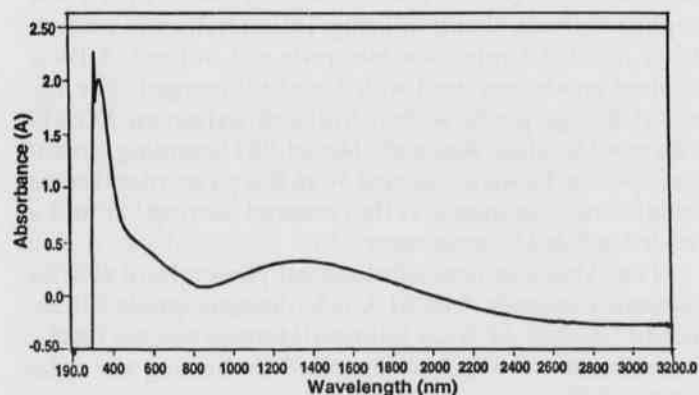Fig. 2. Forward sweep of a voltammogram (current-voltage curve) for an ethylene glycol solution the same as with Fig. 1. Note the cathodic photocurrent pulses centered at -0.5 V.

Fig. 3. X-ray diffraction pattern for a film deposited at -0.6 V from the solution described by Fig. 1 and Fig. 2. Note the matches with peak locations for CdTe powder; (i.e., File 15-770).

Fig. 4. Optical obsorbance vs. wavelength curve for the same film as with Fig. 3. Note the absorption edge near 800 nm.

respectively, consistent with previous data presented for polycrystalline CdTe. The absorbance "tail" tapering down toward wavelengths greater than 800 nm could reflect slight Te-richness. This shows that the correlation of E_{oc} versus E_{sweep} plots with CdTe deposition voltage remains for a change in [Te(IV)].

The last data set presented reveals a change in phase correlating with the corresponding E_{oc} change. Figure 13 is a photovoltammogram for a solution containing $1 \cdot 10^{-4}$ M $TeCl_4$. The Te plating currents are relatively small for this lower concentration solution. Figure 14 is an E_{oc} versus E_{sweep} plot for the solution. Low currents cause the Te plating rate to be slow and the E_{oc} "plateau" for elemental Te is not at all level. This is a direct result of the fact that the Te current is nearly diffusion-limited and the Te(IV) concentration steadily decreases toward zero at the cath-
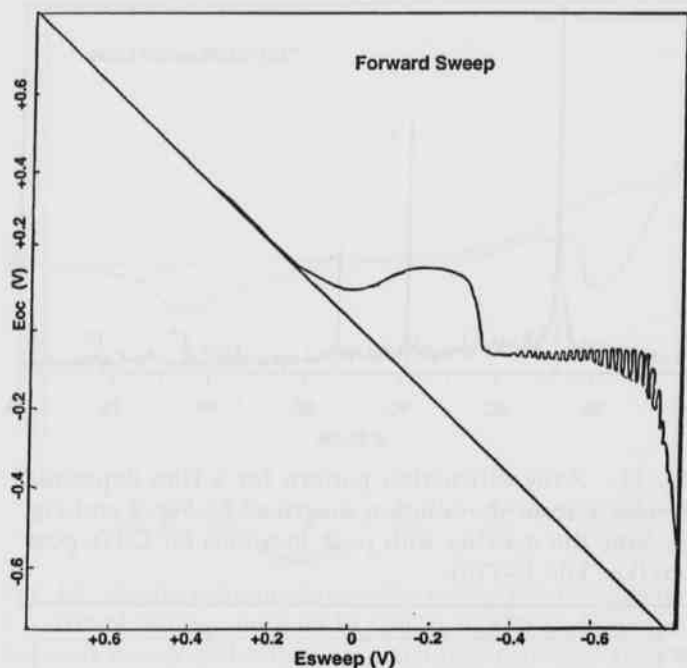
Fig. 5. E_{oc} vs. E_{sweep} curve for an ethylene glycol solution containing $5 \cdot 10^{-4}$ M TeCl$_4$ and 0.05 M CdCl$_2$ at 100°C. Note the cathodic photovoltage pulses centered at -0.05 V.
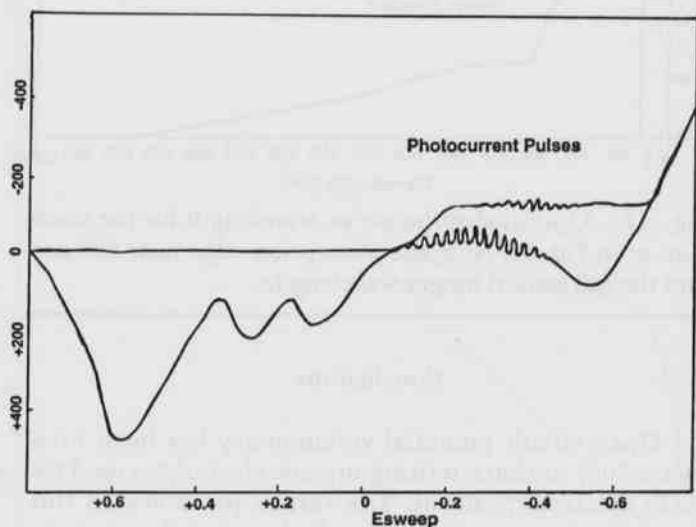

Fig. 6. Cyclic voltammogram for the same solution as in Fig. 5. Note the cathodic photocurrent pulses centered at -0.5 V on the forward sweep.
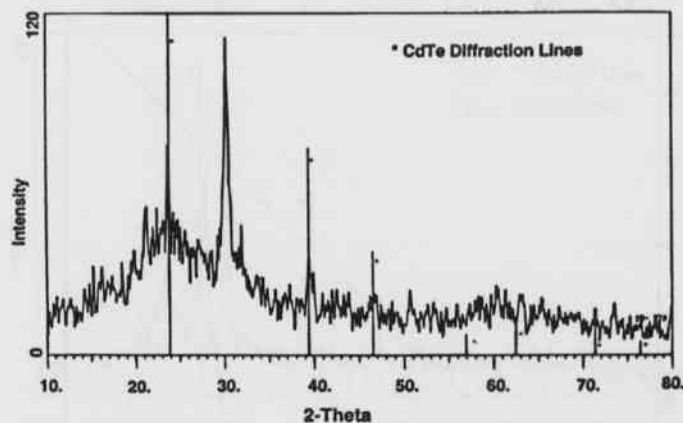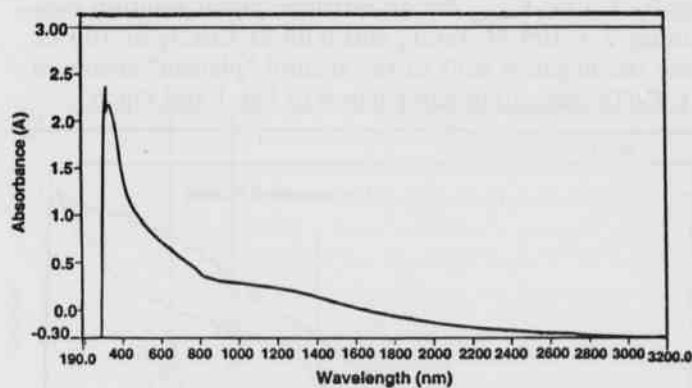

Fig. 7. X-ray diffraction pattern for a film deposited at -0.65 V from the solution described in Fig. 5 and Fig. 6. Note the matches with the peak locations for CdTe powder; (i.e.; File 15-770).

Fig. 8. Optical absorbance vs. wavelength spectrum for the same film as in Fig. 7. Note the absorption edge near 800 nm.

ode surface as the sweep voltage sweeps negative. The most positive plateau structure on the potential plot occurs at an E_{sweep} value (i.e. about -0.20 V) corresponding to a sharp rise in current on the cyclic voltammogram. Photocurrents are not observed, however, until the E_{sweep} value is negative of -0.58 V. At this voltage, a small transition is observed on the E_{oc} versus E_{sweep} plot. A film was deposited at a deposition voltage (i.e. at -0.55 V) just positive of this value.

Figure 15 exhibits XRD data for this film. Notice that the CdTe diffraction peaks are weaker than strong Te diffraction peaks. Figure 16 is a plot of XRD data for a film deposited at -0.65 V which corresponds to the region negative of the transition at -0.58 V. This data reveals a strong diffraction pattern corresponding to CdTe. The absence of Te diffraction peaks indicates that the small
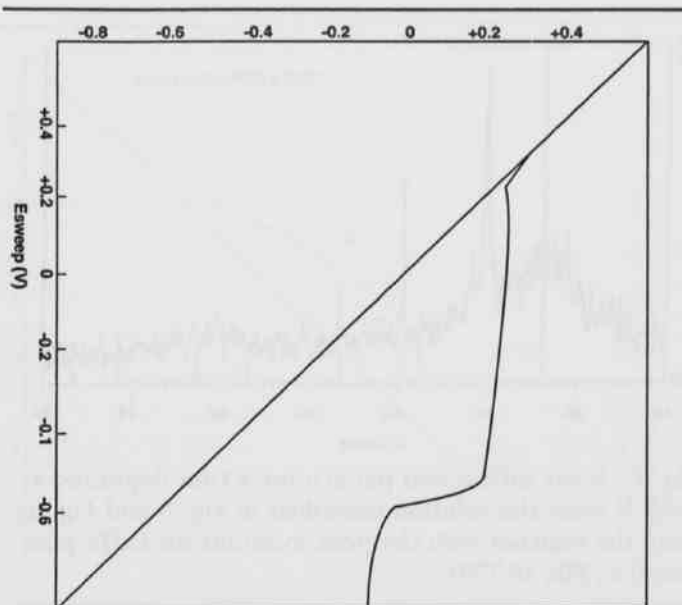
Brandon Kemp, Robert Engelken, Arif Raza, Arees Siddiqui and Omer Mustafa

Fig. 9. E_{oc} vs. E_{sweep} for an ethylene glycol solution containing $7 \cdot 10^{-4}$ M $TeCl_4$ and 0.05 M $CdCl_2$ at 100°C. Note the negative shift of the second "plateau" structure (i.e. CdTe plateau) in comparison to Fig. 1 and Fig. 5.
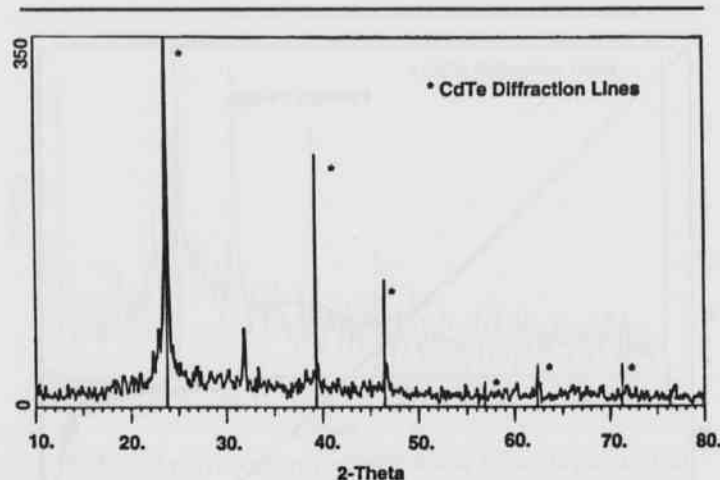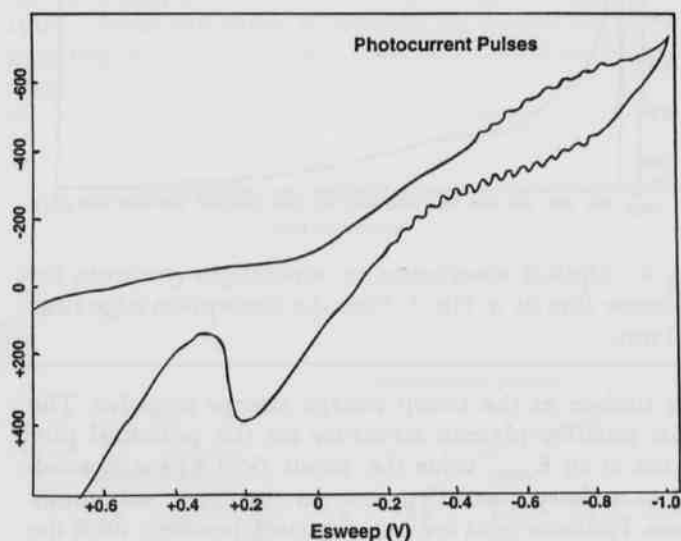
Fig. 10. Cyclic voltammogram for the same solution as in Fig. 9. Note the negative shift of the forward sweep cathodic photocurrent pulses as compared with Fig. 2 and Fig. 6.

transition region observed on the E_{oc} versus E_{sweep} plot again corresponds to a change in deposited phase with respect to deposition voltage.

Fig. 11. X-ray diffraction pattern for a film deposited at -0.85 V from the solution described by Fig. 9 and Fig. 10. Note the matches with peak locations for CdTe powder; (i.e., File 15-770).
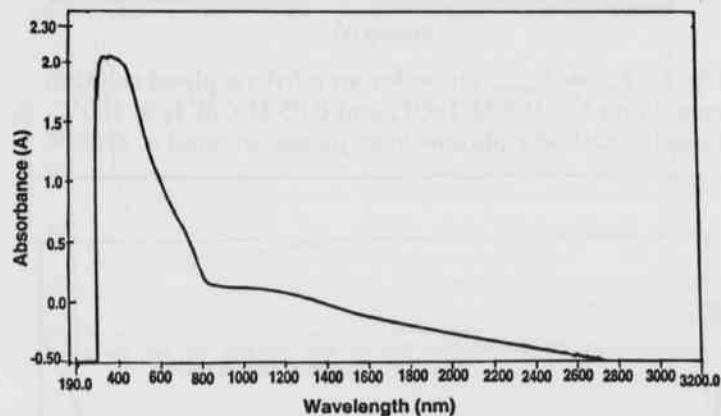
Fig. 12. Optical absorbance vs. wavelength for the same film as in Fig. 11. Note the absorption edge near 800 nm and the tail toward longer wavelengths.

Conclusions

Open circuit potential voltammetry has been used successfully in characterizing organic electrolytes used for CdTe electrodeposition. The results presented in this paper clearly support initial predictions that the open circuit potential can be used to monitor electrodeposited film phase as a function of deposition voltage. Photovoltages observed with rest potential voltammetry correspond to photocurrents on photovoltammograms, and, thus, correlate with the range in which semiconducting material is being plated. Also, spectrophotometer and XRD data for films deposited from the baths demonstrate the potential of this technique for controlling semi-
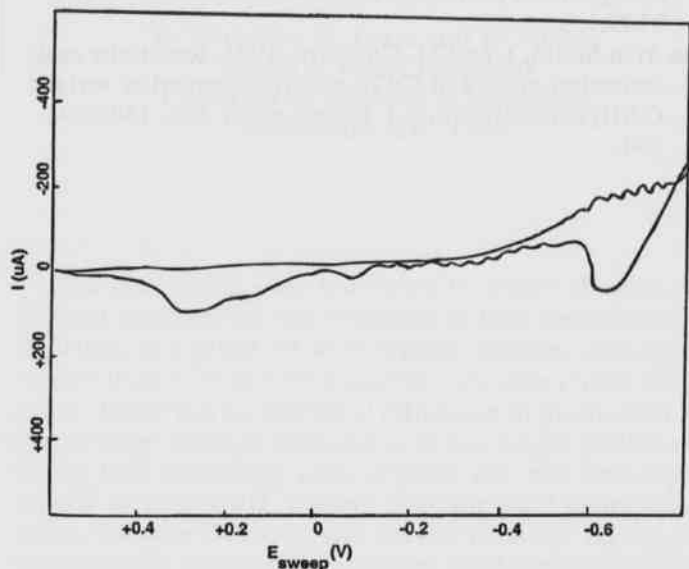
Fig. 13. Cyclic voltammogram for a solution containing $1 \cdot 10^{-4}$ M $TeCl_4$ and 0.05 M $CdCl_2$ at 100°C. Note the forward sweep cathodic photocurrents centered near -0.58 V
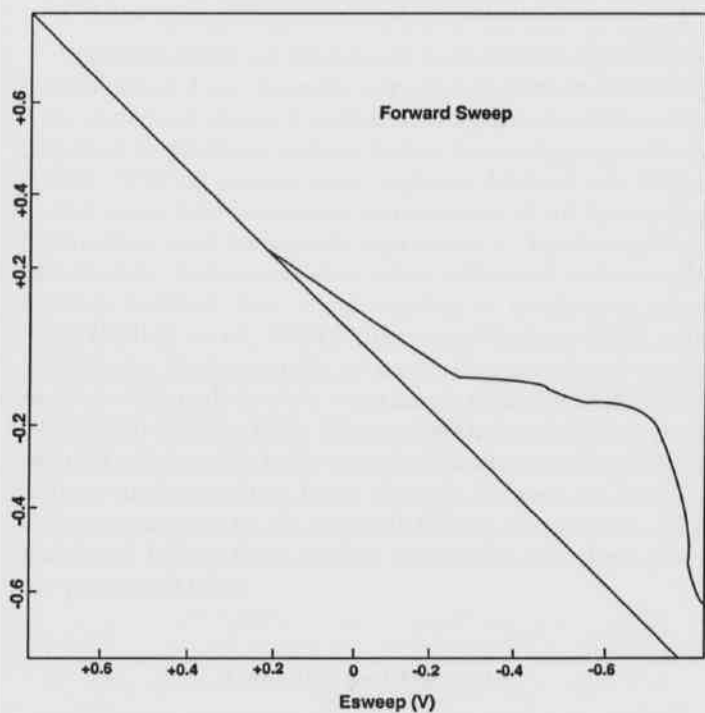

Fig. 14. E_{oc} vs. E_{sweep} for the same solution as in Fig. 13. Note the small transition centered near -0.58 V which corresponds to the onset of forward sweep cathodic photocurrents in Fig. 13.
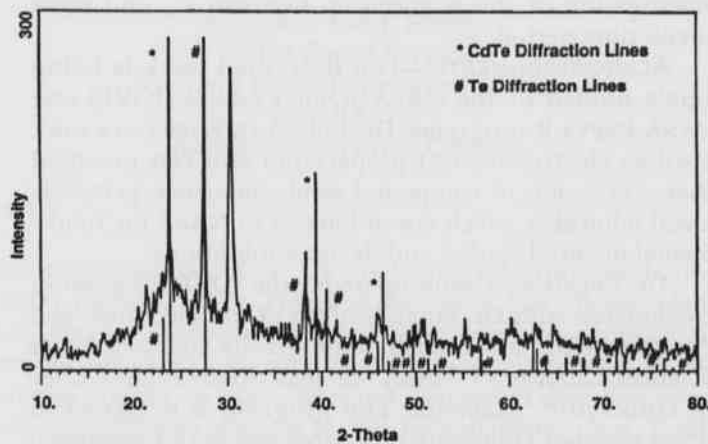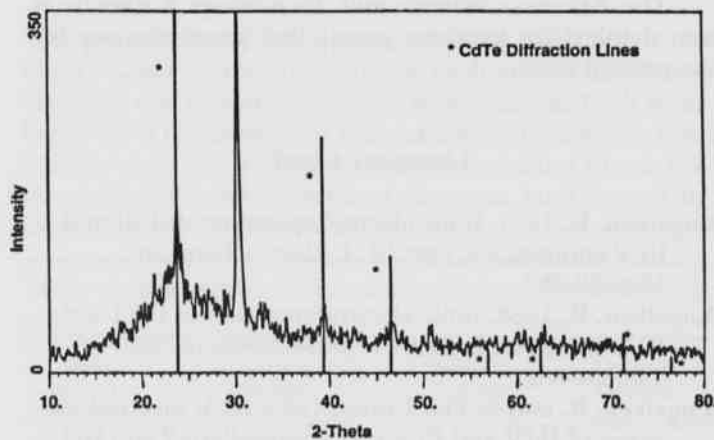

Fig. 15. X-ray diffraction for a film deposited at -0.55 V from the solution described by Fig. 13 and Fig. 14. Note the matches with peak locations for CdTe powder; (i.e., File 15-770) and Te; (i.e., File 36-1452).

Fig. 16. X-ray diffraction for a film deposited at -0.65 V from the solution described by Fig. 13 and Fig. 14. Note the matches with peak locations for CdTe powder; (i.e., File 15-770).

conductor efficacy. Thus, rest potential voltammetry has emerged as a sensitive *in-situ* monitoring technique for use in electrodeposition of semiconductor thin films.

Future work will involve open circuit potential voltammetry for related II-VI compounds such as ZnSe, $Hg_{1-x}Cd_xTe$, and $Hg_{1-x}Zn_xTe$. The application of open circuit potential voltammetry to ternary compounds introduces an intriguing scientific challenge due to the possible existence of multiple compound phases (and, hence, multiple E_{oc} plateau structures) in addition to the pure

elements. Also, future plans include a more quantitative investigation of the relationship between E_{oc} and open circuit time period.

Literature Cited

Engelken, R. 1987. Ionic electrodeposition of II-VI and III-V compounds: Part III. J. Electrochem. Soc. 134:832-837.

Engelken, R. 1988. Ionic electrodeposition of II-VI and III-V compounds: Part IV. J. Electrochem. Soc. 135:834-839.

Engelken, R. and T. Van Doren. 1985. Ionic electrodeposition of II-IV and III-V compounds-Parts I and II. J. Electrochem. Soc. 132:2904-2919.

Ham, D., K. Mishra and K. Rajeswar. 1991. Anodic electrosynthesis of cadmium selenide thin films. J. Electrochem. Soc. 138:100-108.

Kim, H., D. Kim, K. Cho, B. Ahn and H. Im. 1994. Photovoltaic properties of sintered CdS/CdTe solar cells with an indiumin-oxide electrode. J. Electrochem. Soc. 141:3572-3576.

Mori, E., K. Mishra and K. Rajeshwar. 1990. A voltammetric study of compound formation in the Hg-Cd-Te system. J. Electrochem. Soc.137:1100-1106.

Sella, C., P. Boncorps and J. Vedel. 1986. The electrodeposition mechanism of CdTe from acidic aqueous solutions. J. Electrochem. Soc. 133:2043-2047.

Verbrugge, M. and C. Tobias. 1987. Some experimental aspects of the cadmium-tellurium electrochemical codeposition process. J. Electrochem. Soc. 134:3104-3109.

Von Windheim, J. and M. Cocivera. 1991. Resistivity and activation energy of CdTe electrodeposited at various Cd(II) concentrations. J. Electrochem. Soc. 138:250-254.